Spectral characterization of a color scanner by adaptive estimation

Hui-Liang Shen and John H. Xin

Institute of Textiles and Clothing, The Hong Kong Polytechnic University, Hong Kong, China

Received November 6, 2003; revised manuscript received February 25, 2004; accepted March 1, 2004

A new method of spectral characterization for color scanners by the use of adaptive estimation is proposed. It deals with estimation of high-dimensional reflectance vectors from low-dimensional scanner response vectors when the scanner departs from linearity. We first investigate the spectral linearity of the scanner, and then estimate the spectral reflectance adaptively based on the local statistics of a set of neighboring training samples. As the proposed characterization method does not utilize the mathematically recovered spectral responsivity, its inherent inaccuracy is not critical to the spectral characterization. Experimental results showed significant advantage of adaptive estimation when compared with other methods. © 2004 Optical Society of America

OCIS codes: 330.1710, 330.1730.

1. INTRODUCTION

With the rapid development of computer-based image processing techniques, color images are widely used in visualization, communication, and reproduction.[1] It is known that different color devices have their own characteristics, which makes color communication and reproduction difficult. To record and process color images faithfully, techniques of device characterization need to be applied to minimize the impact of device limitations and differences, and preserve color information during the communication of the images between devices.

Device characterization techniques can be classified into two categories: colorimetric and spectral. Colorimetric characterization transforms the imaging device responses, or RGB values, into device-independent CIE tristimulus values.[2–7] Typical techniques used for colorimetric characterization are least-squares-based polynomial regression,[2,3] lookup table with interpolation and extrapolation,[4,5] and artificial neural networks.[6,7] Although these techniques work well, they all suffer from a problem of metamerism. As a consequence, they are constrained to a specific illuminant and observer. To overcome this problem, spectral characterization, which recovers the spectral reflectance from imaging device responses, has received considerable attention recently.[8–13] The spectral sensitivity (or responsivity) of the imaging device plays an important role in spectral characterization. As it is impractical and expensive to measure the sensitivity of a camera or a scanner, some researchers have tried to estimate it mathematically by using various methods such as principal eigenvector analysis,[8,9] set theoretic estimation,[8,10] quadratic programming,[11] Wiener estimation,[12] and parametric model fitting.[13] Based on the recovered spectral sensitivity of a color scanner, Shi and Healey[14] proposed a characterization method that uses a high-dimensional linear reflectance model (LRM) and found that it significantly outperformed the colorimetric polynomial regression method. DiCarlo and Wandell[15] introduced absolute- and relative-scale submanifold estimation methods to improve further the spectral characterization results when the training color sample set systematically deviates from a normal distribution. Haneishi *et al.*[16] estimated the spectral reflectance of art paintings by taking into account the noise distribution and the subdivision of sensor response space. Imai and Berns[17] comparatively investigated the accuracy of spectral reflectance in various spaces by use of principal component analysis. In almost all these techniques[14–17] it was assumed that the spectral sensitivities of the imaging system were measured or mathematically recovered accurately. However, for a real scanner, as the spectral sensitivity may depart considerably from the linear reflectance model,[9] one cannot ensure that these techniques work in spectral characterization when the mathematically recovered sensitivity is not accurate enough.

This paper proposes a new technique to estimate high-dimensional spectral reflectance from low-dimensional scanner responses based on adaptive estimation (AE). In this study, we first investigate scanner linearity by recovering the scanner spectral responsivity with a constrained, linear, least-squares method. Then we calculate the global transform matrix based on the minimum-mean-square-error criterion. Finally, we calculate the local statistics by use of a subset of the neighboring samples and estimate the spectral reflectance. As the recovered scanner spectral responsivity is not used in the proposed AE, the characterization performance will not be affected by its accuracy. Experimental results are also given to evaluate the performance of the proposed technique quantitatively in comparison with other methods.

2. INVESTIGATION OF SCANNER LINEARITY BY RECOVERY OF SPECTRAL RESPONSIVITY

If a color scanner behaves linearly in electronic imaging, the response of the kth ($k = 1, 2, 3$ for three-color-

1084-7529/2004/071125-06$15.00

channel scanners) sensor at a pixel can be given as[18]

$$\nu_k = \int_{\lambda_L}^{\lambda_H} f_k(\lambda) d(\lambda) r(\lambda) l_s(\lambda) \mathrm{d}\lambda + n_k = \int_{\lambda_L}^{\lambda_H} m_k(\lambda) r(\lambda) \mathrm{d}\lambda + n_k, \quad (1)$$

where $f_k(\lambda)$ is the spectral transmittance of the kth color filter, $d(\lambda)$ is the spectral sensitivity of the detector in the measurement, $r(\lambda)$ is the spectral reflectance of the object being scanned, $l_s(\lambda)$ is the spectral radiance of the scanner illuminant, and n_k is a constant bias response. The low and high limits λ_L and λ_H are the wavelength limits beyond which the spectral response of the sensor is zero. As the filter transmittance, sensor sensitivity, and illuminant radiance are unknown for a common scanner, it is convenient to group them into one quantity $m_k(\lambda) = f_k(\lambda) d(\lambda) l_s(\lambda)$, which we refer to as scanner spectral responsivity in this study. In Eq. (1), the indices expressing spatial coordinates are omitted for simplicity.

For practical computation, the continuous functions may be replaced by their sampled counterparts to obtain summation as numerical approximations to integral. If N uniformly spaced samples are used over the spectrum range $[\lambda_L, \lambda_H]$, Eq. (1) can be rewritten with matrix vector notation as

$$\mathbf{v} = \mathbf{M}\mathbf{r} + \mathbf{n}, \quad (2)$$

where $\mathbf{v}$ is the 3×1 vector of scanner responses, $\mathbf{M}$ is the $3 \times N$ matrix of $m_k(\lambda)$, $\mathbf{r}$ is the 3×1 vector of object reflectance, and $\mathbf{n}$ is the 3×1 vector of n_k.

Equations (1) and (2) assume that the scanner behaves linearly. However, as pointed out by Vora *et al.*[12] the actual response of each channel ρ_k may be subject to an input–output nonlinearity that can be represented by an optoelectronic conversion function $F_k(\cdot)$. Then Eq. (2) becomes

$$\boldsymbol{\rho} = F_k(\mathbf{v}) = F_k(\mathbf{M}\mathbf{r} + \mathbf{n}), \quad (3)$$

where $\boldsymbol{\rho}$ is the 3×1 vector of the actual nonlinear response ρ_k.

In this study, the color scanner Epson GT-10000+ was used for characterization; the color targets used were GretagMacBeth ColorChecker Chart (MCC), GretagMacBeth ColorChecker DC (CDC), Kodak Gray Scale Q-14 (Q14), and Kodak Q60 photographic standard (IT8). These four color targets were sequentially scanned at a resolution of 72 dots per inch. The reflectance data of the colors on targets MCC, CDC, and Q14 were measured by a GretagMacbeth Spectrophotometer 7000A in the visible spectrum of 400 to 700 nm with sampling interval of 10 nm. The reflectance data of color target IT8 were obtained from ftp://ftp.ece.uci.edu/pub/mshi/, which were the same used in the study by Shi and Healey.[14] We clipped the provided IT8 reflectance data from the spectrum range 380–730 nm to 400–700 nm to keep it the same as those of the other color targets.

To examine $F_k(\cdot)$ the mean scanner responses of each gray patch on MCC, CDC, and Q14 were calculated in a center 40×80-pixel area. The mean reflectance values of these color patches were calculated in the spectrum range 440–700 nm because the reflectance in the range 400–430 nm is not very flat. The inverse optoelectronic conversion function $F_k^{-1}(\cdot)$ can be regarded as the monotonically increasing nonlinear curve between the actual nonlinear response of the scanner and the mean reflectance values of those gray patches. The functions $F_k^{-1}(\cdot)$ of the blue channel for the color targets MCC, CDC, and Q14 are shown in Fig. 1. The relationships of the red and green channels are quite similar to that of the blue channel. It is noted that the relationships for different color targets are slightly different from each other. This is due mainly to the fact that these color targets are made of materials of different reflection properties. This characteristic is considered by the factor $\mathbf{n}$ in Eq. (3).

After the introduction of the optoelectronic conversion function $F_k(\cdot)$, we then investigated whether the LRM of Eq. (2) can accurately describe the behavior of the scanner. Because of the difficulty in instrumental measurement of the spectral responsivity, we tried to recover it mathematically. In this study, 24 colors on MCC were used to recover the spectral responsivity, and the Q14 was used to obtain nonlinear function $F_k^{-1}(\cdot)$. In the calculation of $\mathbf{M}$, constraints of smoothness, posivitity, and response accuracy were used according to the following inequalities [(4)–(6)]:

$$|2M_k(i) - M_k(i-1) - M_k(i+1)| \leq \epsilon, \quad (4)$$

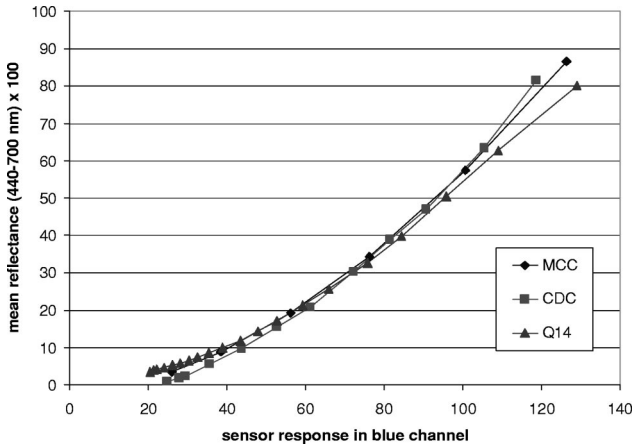

Fig. 1. Reverse nonlinear functions between the sensor response and the mean reflectance of the blue channel for color targets MCC, CDC, and Q14. The relationships of the red and green channels are similar.

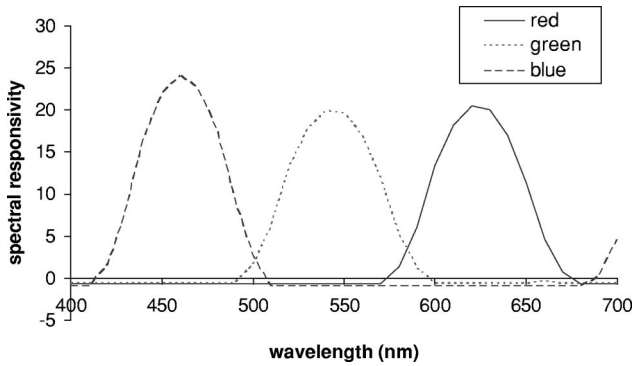

Fig. 2. Recovered spectral responsivity of the scanner using colors on MCC.

Table 1. Comparison of the Actual Linear Responses ν_k and Predicted Ones $\hat{\nu}_k$ by Use of Mathematically Recovered Spectral Responsivity[a]

	MCC			CDC		
Error	Red	Green	Blue	Red	Green	Blue
Mean error (%)	0.80	0.75	1.41	1.88	1.66	2.78
Maximum error (%)	1.90	1.56	4.65	4.70	5.05	9.69

[a] The error of a color is calculated by using $|\nu_k - \hat{\nu}_k|/\nu_{k\,\max} \times 100\%$, where $\nu_{k\,\max}$ is the maximum linear response of the kth channel of the white patch of MCC.

$$\mathbf{M}_k \geqslant \mathbf{0}, \tag{5}$$

$$|\nu_k - \mathbf{M}_k\mathbf{r}| \leqslant \delta, \tag{6}$$

where ϵ and δ are predetermined values, $\mathbf{M}_k$ is the kth ($k = 1, 2, 3$) $1 \times N$ vector of matrix $\mathbf{M}$, and $M_k(i)$ is the ith element of vector $\mathbf{M}_k$. This problem can be regarded as that of the constrained-linear-least-squares and can be solved using standard mathematical methods, such as the routine *lsqlin* in MATLAB. The solved spectral responsivity is shown in Fig. 2, and the calculated $\mathbf{n} = [2.03, 2.41, 1.51]^T$ (T denotes transpose) when $\epsilon = 1.0$ and $\delta = 0.01$ were adopted. As can be seen in Fig. 2, the spectral responsivity at some wavelengths is slightly below 0, which conflicts with relation (5). This is due to the overstringent constraints with the inequalities (4)–(6) for the scanner used, and the spectral responsivity shown in Fig. 2 is the optimal solution under these constraints. Nevertheless, the shape of the responsivity seems quite reasonable. To check the accuracy and generality of responsivity matrix $\mathbf{M}$, the colors on MCC and CDC—except the dark ones (A2, A5, A8, A11, etc.) and the glossy ones (S1-T12) of the CDC target—were used in testing the accuracy of simulated linear scanner response from the measured $\mathbf{r}$ and the recovered $\mathbf{M}$ shown in Eq. (2). The errors between the actual and simulated linear responses are given in Table 1.

As shown in Table 1, the simulation errors of MCC are reasonably low. The errors of the blue channel are slightly larger than those of the red and green channels. However, the mean and standard deviation of the absolute errors of the test target CDC are approximately 2 times larger than those of MCC. This clearly indicates that the recovered spectral responsivity is actually data dependent. It is also considered that the scanner departs from the LRM as the errors for some colors are relatively high.

3. CHARACTERIZATION OF COLOR SCANNER USING ADAPTIVE ESTIMATION

After the mathematical recovery of the spectral responsivity matrix $\mathbf{M}$, the factor $\mathbf{n}$ is also known. If we let $\mathbf{u} = \mathbf{v} - \mathbf{n}$, Eq. (2) can be rewritten as

$$\mathbf{u} = \mathbf{M}\mathbf{r}. \tag{7}$$

The convenient solution to spectral characterization is to estimate the reflectance vector $\hat{\mathbf{r}}$ from the linear response vector $\mathbf{u}$ by an $N \times 3$ matrix $\mathbf{W}$, such that

$$\hat{\mathbf{r}} = \mathbf{W}\mathbf{u}. \tag{8}$$

The estimation of spectral reflectance from linear response can be regarded as determining the linear transform matrix $\mathbf{W}$ in Eq. (8) such that $\hat{\mathbf{r}}$ is a close replica of $\mathbf{r}$ in minimum-mean-squares-error sense. Thus with

$$J = E\{\|\hat{\mathbf{r}} - \mathbf{r}\|^2\}, \tag{9}$$

where E denotes the statistical expectation operator, the problem is to determine the $\mathbf{W}$ that minimizes J. By differentiation of J with respect to $\mathbf{W}$, we get the Wiener–Hopf equation[19]

$$\mathbf{W} = \mathbf{R}_{ru}\mathbf{R}_r^{-1}, \tag{10}$$

where

$$\mathbf{R}_{ru} = E\{\mathbf{r}\mathbf{u}^T\}, \tag{11}$$

$$\mathbf{R}_r = E\{\mathbf{r}\mathbf{r}^T\}, \tag{12}$$

are the cross- and autocorrelation matrices, respectively. An alternative approach to solving $\mathbf{W}$ is to employ the orthogonality principle in the minimization of the mean-squares error; the transform matrix then becomes[20]

$$\mathbf{W} = \mathbf{K}_r\mathbf{M}^T(\mathbf{M}\mathbf{K}_r\mathbf{M}^T)^{-1}, \tag{13}$$

where $\mathbf{K}_r = E\{(\mathbf{r} - E\{\mathbf{r}\})(\mathbf{r} - E\{\mathbf{r}\})^T\}$ is the covariance matrix of $\mathbf{r}$. Equation (13) was usually used in previous studies on multispectral imaging and spectral characterization.[16,17,21] An implicit assumption of this equation is that the spectral responsivity is accurate enough. However, as discussed above, the behavior of a real scanner may depart from the LRM considerably. Therefore, we consider Eq. (10) is much more appropriate as it does not explicitly incorporate the spectral responsivity.

The most straightforward way for estimation of the matrix $\mathbf{W}$ is to use the statistics (correlation matrix) of a large number of training samples. However, the statistics is also inconsistent for individual training samples,[15] especially when a real scanner departs from the LRM. Therefore, in this study, we consider estimating the statistics adaptively according to the candidate color sample for characterization. One possible way is to divide the scanner sensor space into several blocks and estimate the correlation statistics from the data within each block. The drawback of this method is that the estimated transform matrix may fail to describe the statistics of the candidate samples lying at block boundaries. In this study, we propose an AE method consisting of the following steps:

1. Calculate the correlation matrices $\mathbf{R}_r$ and $\mathbf{R}_{ru}$ by using all the training samples and estimating the global transform matrix $\mathbf{W}_0$ according to Eq. (10).
2. For a candidate color sample with known linear response $\mathbf{u}_i$, calculate its reflectance $\mathbf{r}_{i0}$ using the estimated $\mathbf{W}_0$, and then search L neighboring samples (except the candidate sample itself) of $\mathbf{r}_{i0}$ in terms of Euclidean distance in the reflectance space.
3. Estimate the adaptive transform matrix $\mathbf{W}_i$ by using these selected L neighboring training samples and calculating the final reflectance $\mathbf{r}_i$ from the candidate sample $\mathbf{u}_i$.

As the selected L neighboring samples in step (2) are close to the candidate sample $\mathbf{u}_i$, the estimated $\mathbf{W}_i$ will describe its statistics more accurately than $\mathbf{W}_0$ does. An important issue in this method is to decide the value of L, or equivalently, how many training samples are appropriate for the estimation of $\mathbf{W}_i$. It is noted that in deciding the suitable value of L, we always assume that the candidate sample itself is not included in the training samples for the AE.

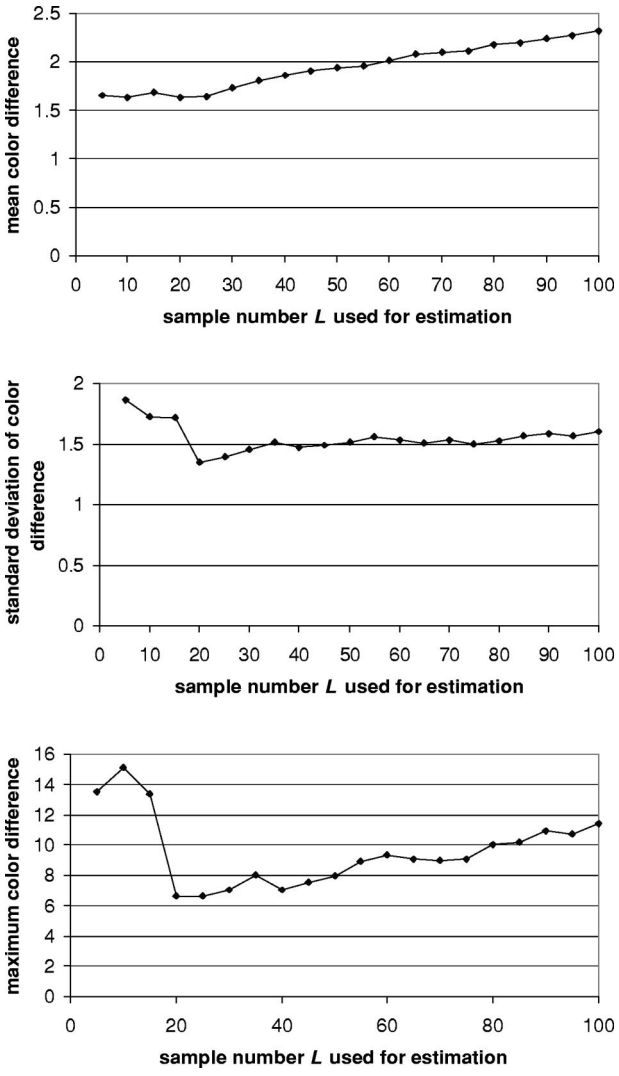

Fig. 3. Relationship between the training sample number L and mean (top), standard deviation (middle), and maximum (bottom) of color difference ΔE_{94}* of CDC.

CIE 1994 color difference ΔE_{94}* under standard illuminant D65 was used to calculate testing results for each color in the CDC target when different L numbers were used. The mean, standard deviation, and maximum of ΔE_{94}* are plotted in Fig. 3. It is found that the mean of the color difference slowly increases with increase in training sample number L. From Fig. 3, we consider $L = 20$ is appropriate for the adaptive estimation for target CDC. We note that the value of L is color-target related. For example, we found $L = 10$ to be appropriate for IT8.

4. EXPERIMENTAL RESULTS

Color targets CDC and IT8 were used for the spectral characterization of the Epson color scanner. For the CDC, we obtain the linear scanner response $\mathbf{u}$ after the recovery of spectral responsivity $\mathbf{M}$ shown in Fig. 2. The reflectance data of IT8 were measured by Gretag Spectroscan and Spectrolino spectrophotometers.[14] Because there may be instrumental disagreement between these two different spectrophotometers, we used the reflectance data of IT8 to obtain the linear response vector $\mathbf{u}$ in estimating the reflectance vector of IT8.

In the quantitative evaluation of the proposed AE method, in addition to ΔE_{94}*, we used the term of rms error defined in the reflectance as

$$\text{rms error} = \left[\frac{(\mathbf{r} - \hat{\mathbf{r}})^T(\mathbf{r} - \hat{\mathbf{r}})}{N}\right]^{1/2}, \tag{14}$$

where N is the sampling number in the visible spectrum and $\mathbf{r}$ and $\hat{\mathbf{r}}$ are measured and estimated spectral reflectance, respectively.

To evaluate the characterization performance of the proposed AE method, we also determined the characterization results by use of the LRM[14] for comparison. A brief description of that method is given in Appendix A for reference. For the LRM, two cases are used for comparison. We assume the candidate is included in the training samples for the first case, while excluded for the second case. We thought the second case would be more realistic for real characterization problems. The nonadaptive estimation (NAE) by Eq. (10) was also conducted for comparison. The comparative evaluation results of these methods are shown in Tables 2 and 3 for color targets CDC and IT8, respectively. Although the performance of the LRM method (candidate sample included) was slightly better than the proposed method, it was thought that, for a realistic characterization problem, it would rarely be the case that the candidate sample itself were in the training sample database. Therefore, it was considered that the proposed AE method significantly outperformed the LRM and NAE methods in terms of both color difference and rms error. For both targets of CDC and IT8, the mean color difference is lower than $1.7\Delta E_{94}$* units, which is considered to be sufficient for many applications.

5. CONCLUSIONS

Spectral characterization consists of calculation of high-dimensional reflectance vectors from low-dimensional re-

Table 2. Mean, Standard Deviation (Std.), and Maximum (Max.) of Color Difference ΔE_{94}* and Rms Error for the LRM Method in Candidate Included (In.) Case and Candidate Excluded (Ex.) Case, NAE, and the Proposed AE for Target CDC

	ΔE_{94}*			Rms Error		
Method	Mean	Std.	Max.	Mean	Std.	Max.
LRM (In.)	1.49	0.97	7.05	0.0130	0.0090	0.0784
LRM (Ex.)	3.11	2.41	13.90	0.0331	0.0227	0.1157
NAE	2.78	2.17	14.82	0.0293	0.0212	0.1488
AE	1.63	1.35	6.59	0.0179	0.0164	0.0931

Table 3. Mean, Standard Deviation (Std.), and Maximum (Max.) of Color Difference ΔE_{94}* and Rms Error for the LRM Method in Candidate Included (In.) Case and Candidate Excluded (Ex.) Case, NAE, and the Proposed AE for Target IT8

	ΔE_{94}*			Rms Error		
Method	Mean	Std.	Max.	Mean	Std.	Max.
LRM (In.)	2.13	1.46	7.29	0.0081	0.0043	0.0267
LRM (Ex.)	2.87	1.98	11.41	0.0138	0.0089	0.0647
NAE	3.05	1.93	8.92	0.0137	0.0072	0.0440
AE	1.44	1.01	5.81	0.0066	0.0047	0.0266

sponse vectors. Although several techniques have been presented for the characterization of imaging devices such as digital cameras and scanners in previous studies, they all assume that the spectral sensitivity (or responsivity) can be accurately measured or recovered mathematically. However, a real scanner may depart considerably from the presumed linear reflectance model. To account for this problem, we have proposed an AE technique to characterize a color scanner. The proposed method first mathematically recovers the spectral responsivity, then adaptively estimates the local statistics of the candidate color sample by searching appropriate training samples. Experimental evaluation indicates that the spectral-characterization-based AE significantly outperforms that based on the LRM in terms of both color difference and rms error. The proposed method has potential applications such as textile quality control and art painting recording where high color accuracy is required.

APPENDIX A: SCANNER CHARACTERIZATION USING LINEAR REFLECTANCE MODEL

According to its relative smoothness, the spectral reflectance $\mathbf{r}$ can be accurately approximated using a series of coefficients a_i and basis functions $\mathbf{b}_i$ as

$$\mathbf{r} = \sum_{i=1}^{K} a_i \mathbf{b}_i = \mathbf{Ba}, \tag{A1}$$

where K is the number of basis functions, $\mathbf{a} = [a_1, a_2, \ldots, a_K]^T$, and $\mathbf{B} = [\mathbf{b}_1, \mathbf{b}_{22}, \ldots, \mathbf{b}_K]$. With the recovered spectral responsivity of the scanner, the linear response can be represented by

$$\mathbf{u} = \mathbf{Mr} = \mathbf{MBa} = \mathbf{MB}_1\mathbf{a}_1 + \mathbf{MB}_2\mathbf{a}_2, \tag{A2}$$

where

$$\mathbf{B}_1 = [\mathbf{b}_1, \mathbf{b}_1, \cdots, \mathbf{b}_{K-3}], \quad \mathbf{B}_2 = [\mathbf{b}_{K-2}, \mathbf{b}_{K-1}, \mathbf{b}_K],$$

$$\mathbf{a}_1 = [a_1, a_2, \cdots, a_{K-3}]^T, \quad \mathbf{a}_2 = [a_{K-2}, a_{K-1}, a_K]^T.$$

We can represent $\mathbf{a}_2$ in terms of $\mathbf{a}_1$ by rearranging Eq. (A2) into

$$\mathbf{a}_2 = (\mathbf{MB}_2)^{-1}(\mathbf{u} - \mathbf{MB}_1\mathbf{a}_1). \tag{A3}$$

Therefore the reflectance becomes

$$\mathbf{r} = \mathbf{B}_1\mathbf{a}_1 + \mathbf{B}_2(\mathbf{MB}_2)^{-1}(\mathbf{u} - \mathbf{MB}_1\mathbf{a}_1). \tag{A4}$$

The solution $\mathbf{r}$ is now constrained by the three-dimensional sensor responses $\mathbf{u}$. By varying the K-3 element of $\mathbf{a}_1$, we obtain a set S_r of reflectance vectors that are consistent with $\mathbf{u}$ and the LRM. The objective is to find the $\mathbf{r}$ in the set S_r that is the most similar in Euclidean distance to a training reflectance vector. For a given training $\mathbf{r}_i$, the reflectance $\mathbf{r}^*$ of S_r that minimizes $\|\mathbf{r} - \mathbf{r}_i\|$ is the solution of a linear least-squares problem:

$$\mathbf{r}_i^* = \mathbf{B}_1\mathbf{a}_1^* + \mathbf{B}_2(\mathbf{MB}_2)^{-1}(\mathbf{u} - \mathbf{MB}_1\mathbf{a}_1^*), \tag{A5}$$

where

$$\mathbf{a}_1^* = [\mathbf{B}_1 - \mathbf{B}_2(\mathbf{MB}_2)^{-1}\mathbf{MB}_1]^+[\mathbf{r}_i - \mathbf{B}_2(\mathbf{MB}_2)^{-1}\mathbf{u}], \tag{A6}$$

and where the superscript + represents pseudoinverse. The error can be calculated as

$$D_i^* = \|\mathbf{r}_i^* - \mathbf{r}_i\|. \tag{A7}$$

The overall minimization of $\mathbf{r}^*$ is given by the $\mathbf{r}_i^*$ corresponding to the minimum D_i^* in all the training samples in the case.

ACKNOWLEDGMENT

The authors acknowledge the financial support of this project from the Hong Kong Polytechnic University and the Research Grants Council of Hong Kong SAR Government (project reference: PolyU 5153/01E).

Corresponding author J. H. Xin can be reached by e-mail at tcxinjh@inet.polyu.edu.hk.

REFERENCES

1. L. W. MacDonald and M. R. Luo, *Color Imaging: Vision and Technology* (Wiley, Chichester, UK, 1999).
2. G. W. Hong, M. R. Luo, and P. A. Rhodes, "A study of digital camera colorimetric characterization based on polynomial modeling," Color Res. Appl. **26**, 76–84 (2001).
3. H. R. Kang, "Color scanner calibration," J. Imaging Sci. Technol. **36**, 162–170 (1992).
4. P. C. Hung, "Colorimetric calibration for scanners and media," in *Camera and Input Scanner Systems*, W. C. Chang and J. R. Milch, eds., Proc. SPIE **1448**, 164–174 (1991).
5. P. C. Hung, "Colorimetric calibration in electronic imaging devices using a look-up-table in interpolations," J. Electron. Imaging **2**, 53–61 (1993).
6. H. R. Kang and P. G. Anderson, "Neural network applications to the color scanner and printer calibrations," J. Electron. Imaging **1**, 125–134 (1992).
7. S. Tominaga, "A neural network approach to color reproduction in color printers," *Proceedings of First IS&T/SID Color Imaging Conference: Transforms and Transportability of Color* (Society for Imaging Science and Technology, Springfield, Va., 1993), pp. 173–177.
8. G. Sharma and H. J. Trussell, "Characterization of scanner sensitivity," *Proceedings of First IS&T/SID Color Imaging Conference: Transforms and Transportability of Color* (Society for Imaging Science and Technology, Springfield, Va., 1993), pp. 103–107.
9. J. E. Farrell and B. A. Wandell, "Scanner linearity," J. Electron. Imaging **2**, 225–230 (1993).
10. G. Sharma and H. J. Trussell, "Set theoretic estimation in color scanner characterization," J. Electron. Imaging **5**, 479–489 (1996).
11. K. Barnard and B. Funt, "Camera characterization for color research," Color Res. Appl. **27**, 152–163 (2002).
12. P. L. Vora, J. E. Farrell, J. D. Tietz, and D. H. Brainard, "Image capture: simulation of sensor responses from hyperspectral images," IEEE Trans. Image Process. **10**, 307–316 (2001).
13. M. Thomson and S. Westland, "Colour-imager characterization by parametric fitting of sensor responses," Color Res. Appl. **26**, 442–449 (2001).
14. M. Shi and G. Healey, "Using reflectance models for color scanner calibration," J. Opt. Soc. Am. A **19**, 645–656 (2002).
15. J. M. Dicarlo and B. A. Wandell, "Spectral estimation theory: beyond linear but before Bayesian," J. Opt. Soc. Am. A **20**, 1261–1270 (2003).
16. H. Haneishi, T. Hasegawa, A. Hosoi, Y. Yokoyama, N. Tsumura, and Y. Miyake, "System design for accurately estimating the spectral reflectance of art paintings," Appl. Opt. **39**, 6621–6632 (2000).
17. F. H. Imai and R. S. Berns, "A comparative analysis of spectral reflectance estimation in various spaces using a trichromatic camera system," J. Imaging Sci. Technol. **44**, 280–287 (2000).
18. G. Sharma and H. J. Trussell, "Digital color imaging," IEEE Trans. Image Process. **6**, 901–932 (1997).
19. M. H. Hayes, *Statistical Digital Signal Processing and Modeling* (Wiley, New York, 1996).
20. W. K. Pratt, *Digital Image Processing*, 2nd ed. (Wiley, New York, 1991).
21. Y. Murakami, T. Obi, M. Yamaguchi, N. Ohyama, and Y. Komiya, "Spectral reflectance estimation from multi-band image using color chart," Opt. Commun. **188**, 47–54 (2001).